Inhibition of Copper Corrosion by 2-Aminobenzenethiol in Aerated 2 M HNO₃ Medium

A. Zarrouk[1,], H. Zarrok[2], R. Salghi[3], B. Hammouti[1] Eno E. Ebenso[4], F. Bentiss[5], H. Oudda[2], M. Elbakri[6], R. Touir[6]*

[1] LCAE-URAC 18, Faculty of Science, University of Mohammed Premier, Po Box 717 60000 Oujda, Morocco
[2] Laboratory Separation Processes, Faculty of Science, University Ibn Tofail PO Box 242, Kenitra, Morocco.
[3] Laboratory of Environmental Engineering and Biotechnology, ENSA, University Ibn Zohr, PO Box 1136, 80000 Agadir, Morocco.
[4] Department of Chemistry and Material Science Innovation & Modelling (MaSIM) Research Focus Area, Faculty of Agriculture, Science and Technology North-West University (Mafikeng Campus), Private Bag X2046, Mmabatho 2735, South Africa,
[5] Laboratoire de Catalyse et de Corrosion des Matériaux (LCCM), Faculté des Sciences, Université Chouaib Doukkali, B.P. 20, M-24000 El Jadida, Morocco
[6] Materials, Electrochemical and Environment Laboratory, Faculty of Science, University Ibn Tofail, BP 133, Kenitra, Morocco.
[*]E-mail: azarrouk@gmail.com

Effect of 2-aminobenzenethiol (ABT) on copper corrosion as a corrosion inhibitor in an aerated acidic solution of 2 M HNO₃ has been investigated using gravimetric and electrochemical techniques. A significant decrease in the corrosion rate of copper was observed in the presence of the investigated organic compound. The potentiodynamic polarization data indicated that the inhibitor was of mixed type. Impedance measurements showed that the charge transfer resistance increased and double layer capacitance decreased with increase in the inhibitor's concentration. Adsorption of ABT molecules on copper surface was found to obey the Langmuir adsorption isotherm. Also, some thermodynamic data for the adsorption and dissolution processes are calculated and discussed. Results obtained from potentiodynamic polarization, impedance measurements and gravimetric method are in good agreement.

1. INTRODUCTION

Corrosion is one of the major problems encountered in the industrial application of materials. Millions of dollars are spent by the oil industry, for instance, on the prevention of corrosion process in metals. Among the procedures used to prevent corrosion, the use of inhibitors is the most common, given that it presents some advantages of economical and environmental nature, as well as great efficiency and high applicability. It is well known that organic molecules containing heteroatoms act efficiently as corrosion inhibitors [1-18]. Organic compounds containing functional electronegative groups and π electrons in triple or conjugated double bonds such as nitrogen, sulfur, and oxygen are usually good inhibitors since these compounds are easily adsorbed on metal surfaces [19-26]. The adsorption of these compounds are also influenced by the electronic structure of inhibiting molecules, steric effect, aromaticity and electron density at donor site, presence of a functional group such as -CHO, -N=N, R-OH, etc., molecular area and molecular weight of the inhibitor molecule [27-30].

In the present work, the inhibition effect of ABT on the corrosion of copper in 2 M HNO_3 solution at 303-343K was studied using weight loss, potentiodynamic polarisation curves and electrochemical impedance spectroscopy (EIS) methods. The adsorption isotherm of inhibitor on copper surface was determined. Both standard thermodynamic parameters (standard adsorption free energy (ΔG_{ads}^{o}), standard adsorption enthalpy (ΔH_{ads}^{o}) and standard adsorption entropy (ΔS_{ads}^{o})) and kinetic parameters (apparent activation energy E_a and pre-exponential factor k) are calculated and discussed in detail. A probable inhibitive mechanism is presented from the viewpoint of adsorption.

2. EXPERIMENTAL METHODS

2.1. Materials

The investigated amine, namely 2-aminobenzenethiol (ABT) is obtained from Sigma-Aldrich chemical co. and its chemical structure is presented in Fig. 1. The concentration range of the tested inhibitor employed in the inhibition study was 1×10^{-6} M to 1×10^{-3} M.
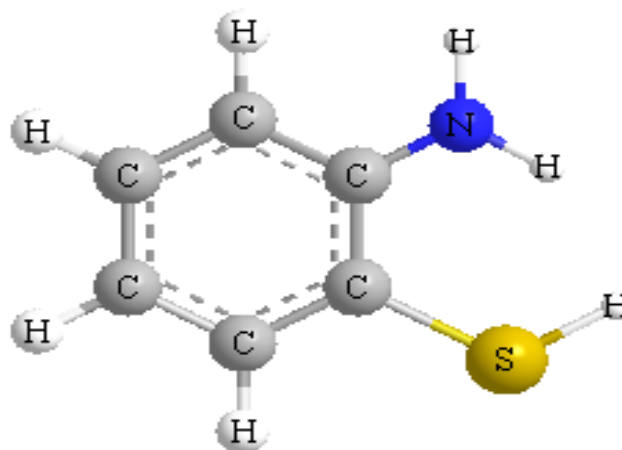
Figure 1. The molecular structure of 2-aminobenzenethiol (ABT).

The material used in this study is a copper with a chemical composition (in wt%) of 0.01 % Ni, 0.019 % Al, 0.004 % Mn, 0.116 % Si and 99.5 % Cu Prolabo Chemicals. Prior to all measurements, the copper samples were pre-treated by grinding with emery paper SiC (180, 600, 1200 and 2000); rinsed with distilled water, degreased in ethanol in an ultrasonic bath immersion for 5 min, washed again with bidistilled water and then dried at room temperature before use. The acid solutions (2 M HNO_3) were prepared by dilution of an analytical reagent grade 65% HNO_3 with doubly distilled water.

2.3. Measurements

2.3.1. Weight loss measurements

Gravimetric measurements were carried out at definite time interval of 1 h at room temperature using an analytical balance (precision ± 0.1 mg). The copper specimens used have a rectangular form (length = 2.0 cm, width = 2.0 cm, thickness = 0.2 cm). Gravimetric experiments were carried out in a double glass cell equipped with a thermostated cooling condenser containing 50 mL of non-de-aerated test solution. After immersion period, the copper specimens were withdrawn, carefully rinsed with bidistilled water, ultrasonic cleaning in acetone, dried at room temperature and then weighted. Triplicate experiments were performed in each case and the mean value of the weight loss was calculated.

2.3.2. Electrochemical measurements

Electrochemical experiments were conducted using impedance equipment (Tacussel-Radiometer PGZ 100) and controlled with Tacussel corrosion analysis software model Voltamaster 4. A conventional three-electrode cylindrical Pyrex glass cell was used. The temperature was thermostatically controlled. The working electrode was copper with the surface area of 0.28 cm^2. A saturated calomel electrode (SCE) was used as a reference. All potentials were given with reference to this electrode. The counter electrode was a platinum plate of surface area of 1 cm^2. A saturated calomel electrode (SCE) was used as the reference; a platinum electrode was used as the counter-electrode. All potentials are reported *vs*. SCE. All electrochemical tests have been performed in aerated solutions at 303 K.

For polarization curves, the working electrode was immersed in a test solution during 30 min until a steady state open circuit potential (E_{ocp}) was obtained. The polarization curve was recorded from -150 to +150 mV/SCE with a scan rate of 1 mV s^{-1}. AC impedance measurements were carried-out in the frequency range of 100 kHz to 10 mHz, with 10 points per decade, at the rest potential, after 30 min of acid immersion, by applying 10 mV ac voltage peak-to-peak. Nyquist plots were made from these experiments. The best semicircle was fit through the data points in the Nyquist plot using a non-linear least square fit so as to give the intersections with the *x*-axis.

3. RESULTS AND DISCUSSION

3.1. Effect of concentration inhibitor

3.1.1. Polarization curves

Fig. 2 represents the potentiodynamic polarization curves of copper in 2 M HNO_3 in the absence and presence of various concentrations of the compounds. Table 1 gives the electrochemical parameters, i.e. corrosion potential (E_{corr}), cathodic Tafel slopes (b_c), corrosion current density (I_{corr}), percentage inhibition efficiency (η_p) and corrosion rate. The inhibition efficiency, η_p, was calculated from polarization measurements according to following equation:

$$\eta_p (\%) = \frac{I_{corr} - I_{corr(i)}}{I_{corr}} \times \qquad (1)$$

where I_{corr} and $I_{corr(i)}$ are the corrosion current densities for copper electrode in the uninhibited and inhibited solutions, respectively.
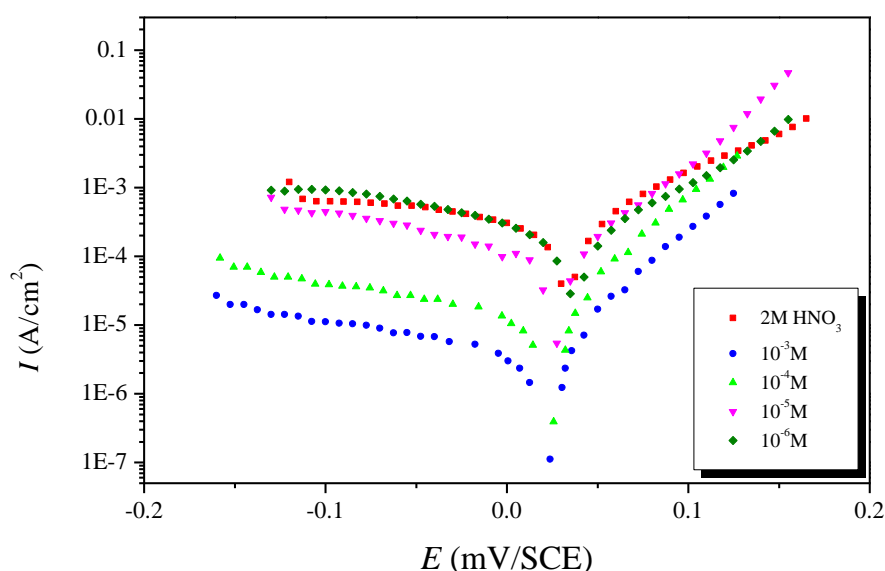
Figure 2. Potentiodynamic polarization curves of copper in 2 M HNO_3 in the presence of different concentrations of ABT at 303 K.

It can be seen from the result that this inhibitor decrease I_{corr} values in the concentration range of 10^{-6}-10^{-3} M concentrations this leads to the increase in the inhibition efficiency by increase in the inhibitor concentration. Maximum reduction of I_{corr} for this inhibitor is obtained at 10^{-3} M. The cathodic Tafel slope (b_c) values show slight changes with the addition of ABT, which suggests that the inhibiting action occurred by simple blocking of the available cathodic sites on the metal surface, which lead to a decrease in the exposed area necessary for oxygen reduction and lowered the

dissolution rate with increasing ABT concentration. It is also observed that E_{corr} values did not change significantly in presence of inhibitor suggesting that the ABT inhibitor is mixed type inhibitor [31].

Based on these results, the action of this compound may be related to adsorption and formation of a barrier film on the copper surface, impeding both cathodic and anodic sites. It is well known that the corrosion of copper in nitric acid involves reduction of the nitrate ion following Eqs. (2) and (3):

$$NO_3^- + 3H^+ + 2e^- \rightarrow HNO_2 + H_2O \qquad (2)$$
$$NO_3^- + 4H^+ + 3e^- \rightarrow NO + 2H_2O \qquad (3)$$

However, in aerated nitric acid solutions, dissolved oxygen may also be reduced on copper surface and this will enable some corrosion to take place [32-34]. It is a good approximation to ignore the hydrogen evolution reaction and only consider oxygen reduction in the aerated nitric acid solutions at potentials near the corrosion potential [35]. Cathodic reduction of oxygen can be expressed either by a direct 4e$^-$ transfer, Eq. (4):

$$O_2 + 4H^+ + 4e^- \rightarrow 2H_2O \qquad (4)$$

or by two consecutive 2e$^-$ steps involving a reduction to hydrogen peroxide first, Eq. (4), followed by a further reduction, according to Eq. (5) [36]:

$$O_2 + 2H^+ + 2e^- \rightarrow 2H_2O_2 \qquad (5)$$
$$H_2O_2 + 2H^+ + 2e^- \rightarrow 2H_2O \qquad (6)$$

Table 1. Polarization parameters and the corresponding inhibition efficiency of copper corrosion in 2 M HNO$_3$ containing different concentrations of ABT at 303 K.

Conc (M)	E_{corr} (mV/SCE)	$-b_c$ (mV/dec)	I_{corr} (μA/cm^2)	η_p (%)
0	34.0	304.7	365.1	——
10^{-3}	24.1	218.2	03.5	99.0
10^{-4}	26.0	240.4	13.5	96.3
10^{-5}	27.0	176.3	89.8	75.4
10^{-6}	36.4	181.5	190.3	47.9

The transfer of oxygen from the bulk solution to the copper/solution interface will strongly affect rate of oxygen reduction reaction, despite how oxygen reduction takes place, either in 4e$^-$ transfer or two consecutive 2e$^-$ transfer steps. Dissolution of copper in nitric acid is described by the following two continuous steps:

$$Cu - e^- \leftrightarrow Cu(I)_{ads} \qquad \text{(fast step)} \qquad (7)$$

$$Cu(I)_{ads} - e^- \leftrightarrow Cu(II) \qquad\qquad\qquad (\text{slow step}) \qquad\qquad (8)$$

where $Cu(I)_{ads}$ is an adsorbed species at the copper surface and does not diffuse into the bulk solution [37-41]. The dissolution of copper is controlled by the diffusion of soluble $Cu(II)$ species from the outer Helmholtz plane to the bulk solution.

3.1.2. Electrochemical impedance spectroscopy measurements

The corrosion behavior of copper in the acidic solution in the absence and presence of inhibitor was also investigated by the EIS method at 303 K. The R_{ct} values were calculated from the difference in impedance at lower and higher frequencies from Nyquist plot (Fig. 3). Using R_{ct} values, the double layer capacitance, C_{dl}, values by using Eq. (9):

$$f(-Zi\,\text{max}) = \frac{1}{2\pi C_{dl} R_{ct}} \qquad\qquad\qquad (9)$$

where f_{max} is the frequency at which the imaginary component of the impedance ($-Z_{max}$) is maximal.

Inhibition efficiency (η_z) can be calculated from Nyquist plot as follows [42];

$$\eta_z(\%) = \frac{1/R_{ct}^0 - 1/R_{ct}}{1/R_{ct}^0} \times 100 \qquad\qquad\qquad (10)$$

where R_{ct}^0 and R_{ct} are the charge-transfer resistance values without and with inhibitor, respectively. The impedance parameters derived from this investigation are given in Table 2. It is worth noting that the presence of inhibitor does not alter the profile of impedance diagrams which are almost semi-circular (Fig. 3), indicating that a charge transfer process mainly controls the corrosion of steel. Deviations of perfect circular shape are often referred to the frequency dispersion of interfacial impedance. This anomalous phenomenon is interpreted by the in homogeneity of the electrode surface arising from surface roughness or interfacial phenomena [43]. In fact, the presence of inhibitor enhances the values of R_{ct} in the acidic solution. On the other hand, the values of C_{dl} decreased with an increase in the inhibitor concentration. This was due to an increase in the surface coverage by this inhibitor, resulting into an increase in the inhibition efficiency. The thickness of the protective layer, dorg, was related to C_{dl} by the following equation [44]:

$$\delta_{org} = \frac{\varepsilon_0 \varepsilon_r}{C_{dl}} \qquad\qquad\qquad (11)$$

where, ε_0 is the dielectric constant and ε_r is the relative dielectric constant. This decrease in the C_{dl}, which can result from a decrease in local dielectric constant and/or an increase in the thickness

of the electrical double layer, suggested that ABT molecules function by adsorption at the metal/solution interface. Thus, the change in C_{dl} values was caused by to the gradual replacement of water molecules by the adsorption of the organic molecules on the metal surface, decreasing the extent of metal dissolution [45].
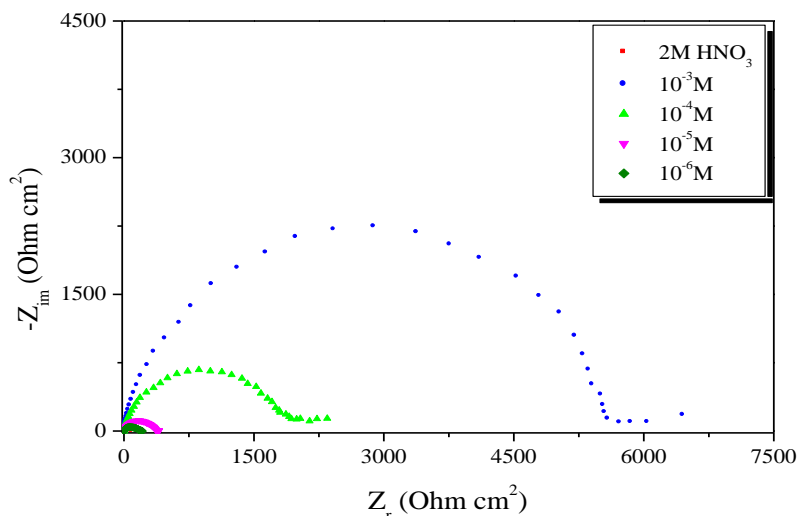
Figure 3. Nyquist diagrams for copper in 2 M HNO_3 containing different concentrations of ABT at 303 K.

Table 2. Impedance parameters and inhibition efficiency values for copper in 2 M HNO_3 containing different concentrations of ABT at 303 K

Conc. (M)	R_{ct} (Ω cm^2)	f_{max} (Hz)	C_{dl} (μF/cm^2)	η_z (%)
0	091.4	15.82	110.1	—
10^{-3}	5630.3	1.25	22.6	98.4
10^{-4}	1877.1	1.58	53.7	95.1
10^{-5}	372.0	7.14	59.9	75.4
10^{-6}	174.7	14.04	64.9	47.7

3.1.3. Weight loss

The inhibition effect of ABT at different concentrations on the corrosion of copper in 2 M HNO_3 solution was studied by weight loss measurements at 303 K after 1 h of immersion period. The corrosion rate (C_R) and inhibition efficiency, η_{WL}(%), were calculated according to the Eqs. 12 and 13 respectively [46]:

$$C_{\mathrm{R}} = \frac{W_{\mathrm{b}} - W_{\mathrm{a}}}{At} \qquad\qquad (12)$$

$$\eta_{\mathrm{WL}}(\%) = \left(1 - \frac{w\mathrm{i}}{w_0}\right) \times 100 \qquad\qquad (13)$$

where W_{b} and W_{a} are the specimen weight before and after immersion in the tested solution, w_0 and w_{i} are the values of corrosion weight losses of copper in uninhibited and inhibited solutions, respectively, A the area of the copper specimen (cm^2) and t is the exposure time (h).

Table 3. Corrosion parameters obtained from weight loss measurements for copper in 2 M HNO_3 containing various concentrations of ABT at 303 K.

Conc. (M)	C_{R} (mg cm^{-2} h^{-1})	η_{WL} (%)
Blank	1.78	—
1×10^{-3}	0.027	98.5
5×10^{-4}	0.073	95.9
1×10^{-4}	0.120	93.2
5×10^{-5}	0.263	85.2
1×10^{-5}	0.460	74.2
1×10^{-6}	0.927	47.9
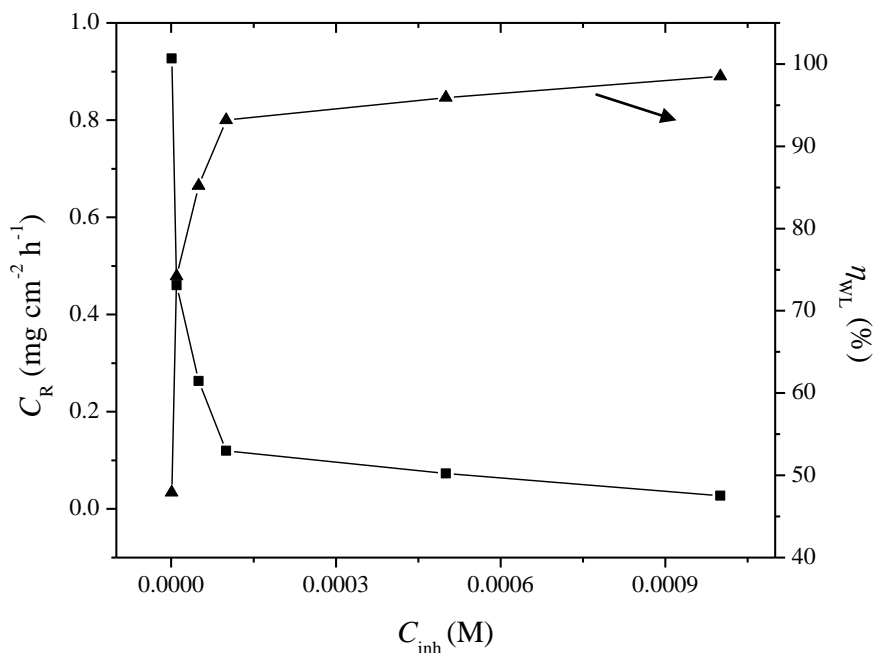
Figure 4. Variation of inhibition efficiency (η_{WL} %) and corrosion rate (C_{R}) in 2 M HNO_3 on copper surface without and with different concentrations of ABT at 303 K.

The values of percentage inhibition efficiency (η_{WL} %) and corrosion rate (C_R) obtained from weight loss method are given in Table 3 and Fig 4. It can be seen that ABT efficiently inhibits the corrosion of copper in 2 M HNO₃ solutions. Data in Table 3 reveal that the inhibition efficiency increases with increasing concentration of ABT. The corrosion inhibition can be attributed to the adsorption of ABT molecules at copper/HNO₃ solution interface [47]. This is due to the presence of hetero atoms like nitrogen and sulphur, and aromatic rings. The extent of inhibition depends upon the nature and mode of adsorption of ABT on the metal surface. The adsorption is assumed to be a quasisubstitution process between the water molecules on the surface and the organic molecules. The interaction of ABT with the metal surface may occur through both the -NH₂ and -SH groups. It is well a known fact that the lone pair of electrons of sulphur and nitrogen is responsible for much predominant adsorption onto the copper surface.

3.2. Effect of temperature

The effect of temperature on the corrosion parameters of copper in free and inhibited solutions of 2 M HNO₃ was studied at a temperature range of 303-343 K. The fractional surface coverage θ can be easily determined from weight loss measurements by the ratio η_{WL}(%) / 100, if one assumes that the values of η_{WL}(%) do no differ substantially from θ. The obtained corrosion parameters are given in Table 4 and show that when temperature increases, the corrosion rate increases in the absence and presence of inhibitor. Data in Table 4 revealed that the investigated of ABT exhibited inhibition properties at all the studied temperatures and the values of inhibition efficiency, η_{WL}(%), decreased with increasing temperature. This can be explained by the decrease of the strength of the adsorption process at elevated temperature and would suggest a physical adsorption mode. The inhibition properties of ABT can also be explained by kinetic model.

The dependence of corrosion rate on the temperature can be regarded as an Arrhenius-type process, the rate of which is given by:

$$C_R = k \exp\left(-\frac{E_a}{RT}\right) \tag{14}$$

where E_a is the apparent activation corrosion energy, R is the universal gas constant and k is the Arrhenius pre-exponential constant. The apparent activation energy values (E_a) at different concentrations of inhibitor were calculated by using the linear regression between $\text{Ln}(C_R)$ and $1/T$ (Fig. 5), and the results are also listed in Table 5. All the linear regression coefficients are close to one, indicating that the copper corrosion in 2 M HNO₃ can be elucidated using the kinetic model. Results in Table 5 show that E_a increases in presence of the inhibitor. The higher values of E_a were obtained in the presence of ABT when compared with those obtained in absence. This could be attributed to their physisorptions on the copper surface [48-50].

Table 4. Corrosion parameters obtained from weight loss for copper in 2 M HNO$_3$ containing various concentrations of ABT at different temperatures

Temperature (K)	Conc. (M)	C_R (mg cm^{-2} h^{-1})	η_{WL} (%)	θ
303	Blank	1.78	—	—
	1×10^{-3}	0.027	98.5	0.985
	5×10^{-4}	0.073	95.9	0.959
	1×10^{-4}	0.120	93.2	0.932
	5×10^{-5}	0.263	85.2	0.852
313	Blank	7.33	—	—
	1×10^{-3}	0.330	95.5	0.955
	5×10^{-4}	0.616	91.6	0.916
	1×10^{-4}	0.837	88.6	0.886
	5×10^{-5}	1.754	76.1	0.761
323	Blank	24.97	—	—
	1×10^{-3}	2.257	91.0	0.910
	5×10^{-4}	3.847	84.6	0.846
	1×10^{-4}	5.793	76.8	0.768
	5×10^{-5}	8.340	66.6	0.666
333	Blank	70.82	—	—
	1×10^{-3}	12.71	82.0	0.820
	5×10^{-4}	19.14	73.0	0.730
	1×10^{-4}	27.08	61.8	0.618
	5×10^{-5}	34.35	51.5	0.515
343	Blank	186.61	—	—
	1×10^{-3}	54.86	70.6	0.706
	5×10^{-4}	77.57	58.4	0.584
	1×10^{-4}	100.15	46.3	0.463
	5×10^{-5}	126.34	32.3	0.323

Kinetic parameters such as enthalpy and entropy of corrosion process may be evaluated from the temperature effect using the transition state theory [51]:

$$C_R = \frac{RT}{Nh} \exp\left(\frac{\Delta S_a}{R}\right) \exp\left(-\frac{\Delta H_a}{RT}\right) \qquad (15)$$

where h is Plank's constant, N is Avogrado's number, ΔS_a is the entropy of activation and ΔH_a is the enthalpy of activation.

Fig. 6 shows a plot of Ln (C_R/T) against $1/T$. A straight lines are obtained with a slope of $(-\Delta H_a/R)$ and an intercept of (ln $R/Nh + \Delta S_a/R$) from which the values of ΔH_a and ΔS_a are calculated, are listed in Table 5. Inspection of these data reveals that the activation parameters (ΔH_a and ΔS_a) of the dissolution reaction of copper in 2 M HNO$_3$ in the presence of ABT were higher than those in the absence of inhibitor (blank). The positive signs of the enthalpy (ΔH_a) reflected the endothermic nature of the copper dissolution process and indicated that the dissolution of copper was difficult [52]. The

entropy of activation ΔS_a in the absence of inhibitor is positive and this value increases positively with the ABT concentration.
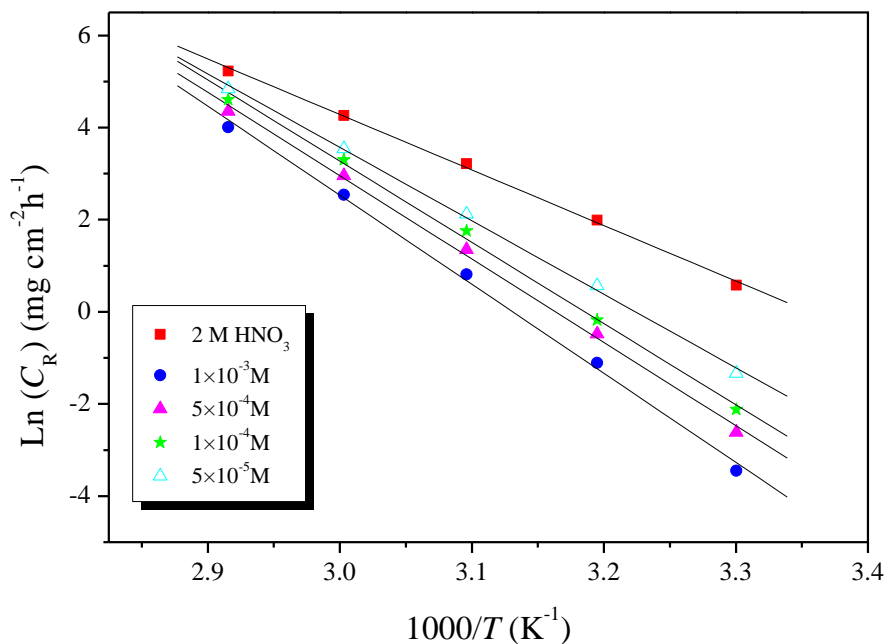
Figure 5. Arrhenius plots for copper corrosion rates (C_R) in 2 M HNO$_3$ in absence and in presence of different concentrations of ABT.

The increase of ΔS_a implies that an increase in disordering takes place on going from reactants to the activated complex [53].
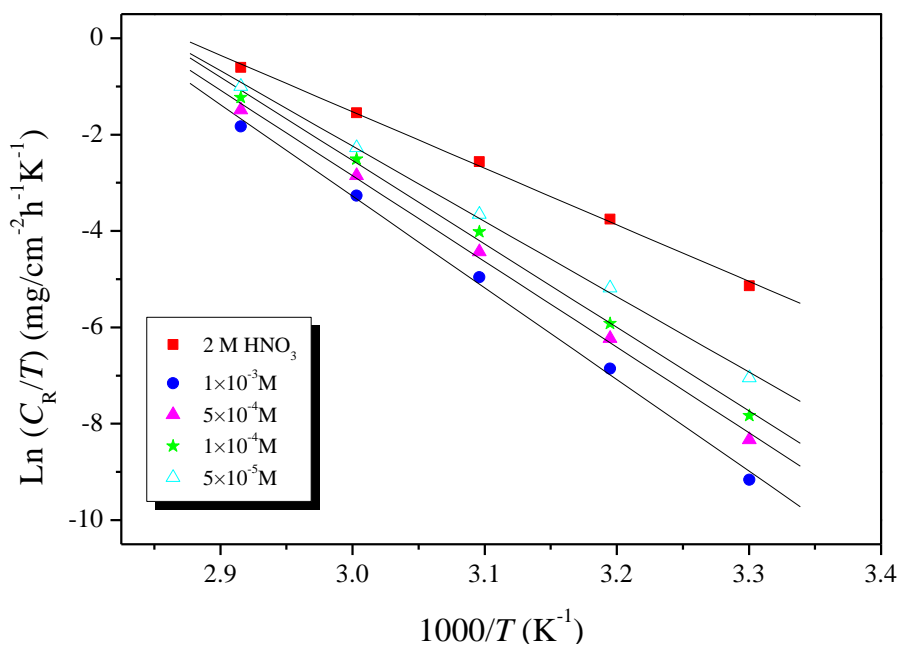
Figure 6. Transition-state plots for copper corrosion rates (C_R) in 2 M HNO$_3$ in absence and in presence of different concentrations of ABT.

Table 5. Corrosion kinetic parameters for copper in 2 M HNO_3 at different concentrations of ABT.

Conc. (M)	k (mg/cm² h)	R^2	E_a (kJ/mol)	ΔH_a (kJ/mol)	ΔS_a (J/mol K)
Blank	3.6627×10^{17}	0.9991	100.21	097.53	082.36
1×10^{-3}	1.9473×10^{26}	0.9986	160.74	158.06	249.40
5×10^{-4}	1.0459×10^{25}	0.9943	151.44	147.75	221.99
1×10^{-4}	2.8971×10^{24}	0.9928	146.83	143.90	213.06
5×10^{-5}	2.1830×10^{22}	0.9974	132.60	129.97	173.75

3.3. Adsorption and thermodynamic considerations

It is a widely held view by many authors that the adsorption of organic inhibitor molecules is often a displacement reaction involving the removal of adsorbed water molecules from the metal surface [54-56]:

$$Org_{(sol)} \quad + \quad X\,H_2O_{(ads)} \quad \rightleftharpoons \quad Org_{(ads)} \quad + \quad X\,H_2O_{(sol)} \qquad (16)$$
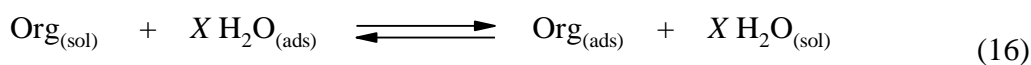
In general, the proceeding of physical adsorption requires the presence of both electrically charged surface of the metal and charged species in the bulk of the solution. Chemisorption process involves charge sharing or charge transfer from the inhibitor molecules to the metal surface to form a coordinate type of a bond. This is possible in case of a positive as well as a negative charge of the metal surface [57].

Perusals of literatures show that organic compounds act as an inhibitor by adsorption on the metal surface. Inhibitor molecules may adsorb on the copper surface in the form of: (*i*) Neutral molecule via chemisorption mechanism involving the sharing of electrons between the heteroatom and copper. (*ii*) Adsorption of inhibitor can occur through π-electron interactions between the aromatic ring of the molecule and the metal surface. (*iii*) Cationic form with positively charged part of the molecule is oriented towards negatively charged copper surface. Adsorption can also occur via electrostatic interaction between a negatively charged surface, which is provided with a specifically adsorbed anion on copper and positive charge of the inhibitor.

The adsorption isotherm experiments were performed to have more insights into the mechanism of corrosion inhibition, since it describes the molecular interaction of the inhibitor molecule with the active sites on the aluminium surface [58]. It is necessary to determine empirically which adsorption isotherm fits best to the surface coverage data in order to use the corrosion rate measurements to calculate the thermodynamic parameters pertaining to inhibitor adsorption. Attempts were made to fit surface coverage values into different adsorption isotherm models. The models considered were [59]:

Temkin isotherm

$$\exp(f.\theta) = K_{ads}C \qquad (17)$$

Langmuir isotherm

$$\theta/(1-\theta) = K_{ads}C \qquad (18)$$

Frumkin isotherm

$$\theta/(1-\theta).\exp(-2f.\theta) = K_{ads}C \qquad (19)$$

and Freundlich isotherm

$$\theta = K_{ads}C \qquad (20)$$

where K_{ads} is the equilibrium constant of the adsorption process, C_{inh} the inhibitor concentration and f the factor of energetic inhomogeneity. By far best results were obtained for Langmuir adsorption isotherm. The correlation coefficient (R^2) was used to choose the isotherm that best fit experimental data (Table 6). The linear relationships of C_{inh}/θ versus C_{inh}, depicted in Fig. 7, suggest that the adsorption of ABT on the copper surface obeyed the Langmuir adsorption isotherm. This isotherm can be represented as:

$$\frac{C_{inh}}{\theta} = \frac{1}{K_{ads}} + C_{inh} \qquad (21)$$

The strong correlation ($R^2 \geq 0.99$) of the Langmuir adsorption for ABT was observed. This isotherm postulates that there is no interaction between the adsorbed molecules and the energy of adsorption is independent on the surface coverage (θ).
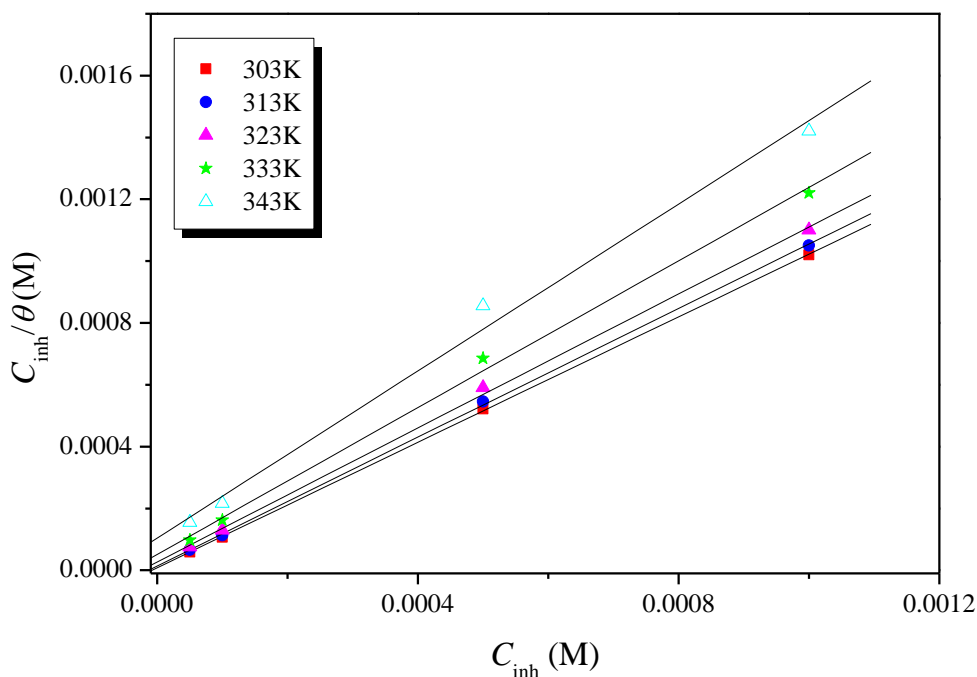
Figure 7. Langmuir's isotherm adsorption model of ABT on the copper surface in 2 M HNO$_3$ at different temperatures.

Langmuir's isotherm assumes that the solid surface contains a fixed number of adsorption sites and each holds one adsorbed species [59]. The slopes of the straight lines obtained from the plots of Langmuir isotherm for ABT are very close to unity, which suggests that the experimental data are well described by Langmuir isotherm and exhibit single-layer adsorption characteristic. The values of equilibrium constant of adsorption K_{ads} obtained from the Langmuir adsorption isotherm are listed in Table 4, together with the values of the Gibbs free energy of adsorption (ΔG^o_{ads}) calculated from the equation:

$$K_{ads} = \frac{1}{55.55} \exp\left(\frac{-\Delta G^o_{ads}}{RT}\right) \qquad (22)$$

where R is gas constant and T is absolute temperature of experiment and the constant value of 55.55 is the concentration of water in solution in mol L^{-1}.

Table 6. Thermodynamic parameters for the adsorption of ABT on the copper in 2 M HNO$_3$ at different temperatures.

Temperature (K)	R^2	K_{ads} (M^{-1})	ΔG^o_{ads} (kJ/mol)	ΔH^o_{ads} (kJ/mol)	ΔS^o_{ads} (J/mol K)
303	0.9999	107384.97	−39.30	−53.98	−48.45
313	0.9998	67407.25	−39.85		−45.14
323	0.9995	36320.05	−38.98		−46.44
333	0.9986	19427.96	−38.46		−46.61
343	0.9961	9498.84	−37.57		−47.84

The high values of K_{ads} for studied ABT indicate stronger adsorption on the copper surface in 2 M HNO$_3$ solution. This can be explained by the presence of sulphur, nitrogen heteroatoms and π-electrons in the inhibitor molecule. It has been reported that the higher the K_{ads} value (>100 M^{-1}), the stronger and more stable the adsorbed layer of the inhibitor on metal surface and consequently, the higher the inhibition efficiency [60]. These data support the good performance of ABT as corrosion inhibitor for copper in 2 M HNO$_3$ solution. The negative values of ΔG^o_{ads}, calculated from Eq. (22), are consistent with the spontaneity of the adsorption process and the stability of the adsorbed layer on the copper surface. Generally, values of ΔG^o_{ads} up to −20 kJ mol^{-1} are consistent with physisorption, while those around −40 kJ mol^{-1} or higher are associated with chemisorption as a result of the sharing or transfer of electrons from organic molecules to the metal surface to form a coordinate bond [61]. In the present study, the calculated values of ΔG^o_{ads} obtained for ABT ranges between −39.30 and −37.57 kJ mol^{-1} (Table 6), indicating that the adsorption of mechanism of ABT on copper in 2 M HNO$_3$ solution at the studied temperatures may be a combination of both physisorption and chemisorption (comprehensive adsorption) [62].

Thermodynamically, ΔG^o_{ads} is related to the standard enthalpy of the adsorption process (ΔH^o_{ads}), via the Gibbs-Helmholtz equation:

$$\left[\frac{\partial(\Delta G^{\circ}_{ads} / T)}{\partial T} \right]_{P} = -\frac{\Delta H^{\circ}_{ads}}{T^{2}} \qquad (23)$$

Eq. (23) can be arranged to give the following equation:

$$\frac{\Delta G^{\circ}_{ads}}{T} = \frac{\Delta H^{\circ}_{ads}}{T} + A \qquad (24)$$

The variation of $\Delta G^{\circ}_{ads}/T$ with $1/T$ gives a straight line with a slope which is equal to ΔH°_{ads} (Fig. 8). It can be seen from this figure that $\Delta G^{\circ}_{ads}/T$ decreases with $1/T$ in a linear fashion. The obtained value of ΔH°_{ads} was -53.98 kJ mol^{-1}. In this case, the standard adsorption entropy (ΔS°_{ads}) values, given in Table 6, can be calculated for all studied systems by applying the following equation:

$$\Delta G^{\circ}_{ads} = \Delta H^{\circ}_{ads} - T \, \Delta S^{\circ}_{ads} \qquad (25)$$

It has been reported that an endothermic adsorption process ($\Delta H^{\circ}_{ads} > 0$) is due to chemisorption while an exothermic adsorption process ($\Delta H^{\circ}_{ads} < 0$) may be attributed to physisorption, chemisorptions or a mixture of both [63]. When the process of adsorption is exothermic, physisorption can be distinguished from chemisorption according to the absolute value of ΔH°_{ads}. For physisorption processes, this magnitude is usually lower than 40 kJ mol^{-1} while that for chemisorption approaches 100 kJ mol^{-1} [64]. In this work, the negative sign of ΔH°_{ads} is an indication that the adsorption of ABT on copper surface is exothermic while its absolute value suggests physisorption.
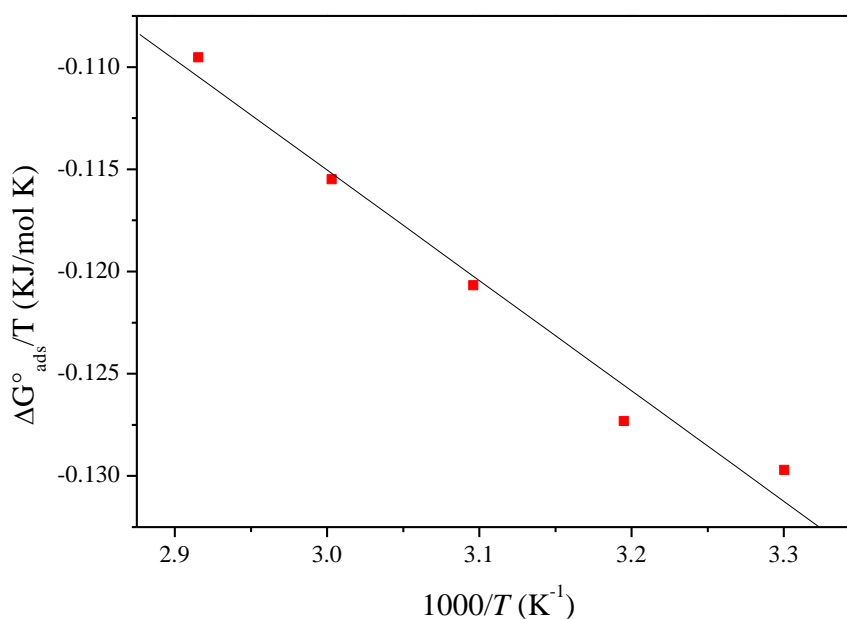
Figure 8. Relationship between $\Delta G^{\circ}_{ads}/T$ and the reverse of absolute temperature.

However, the calculated values of $\Delta G^{\text{o}}_{\text{ads}}$ show that the adsorption of ABT is not merely physical or chemical but a combination of physisorption and chemisorption exists between the inhibitor and the metal surface (comprehensive adsorption) [65]. The negative values of $\Delta S^{\text{o}}_{\text{ads}}$ is generally explained an ordered of adsorbed molecules of inhibitor with the progress in the adsorption onto the copper surface [66].

$\Delta H^{\text{o}}_{\text{ads}}$ and $\Delta S^{\text{o}}_{\text{ads}}$ for the adsorption of ABT on copper surface can be also deduced from the Van't Hoff equation:

$$Ln\, K_{\text{ads}} = -\frac{\Delta H^{\text{o}}_{\text{ads}}}{RT} + \text{constant} \qquad (26)$$

Indeed, a plot of Ln K_{ads} versus $1/T$ gives a straight line, as shown in Fig. 9. The slope of the straight line is $-\Delta H^{\text{o}}_{\text{ads}}/R$ and the intercept is ($\Delta S^{\text{o}}_{\text{ads}}/R + \ln 1/55.55$). The obtained value of $\Delta H^{\text{o}}_{\text{ads}}$ is -52.48 kJ mol^{-1}, confirming the exothermic behaviour of the ABT adsorption on the copper surface. Values of $\Delta H^{\text{o}}_{\text{ads}}$ obtained by the both methods are in good agreement. Moreover, the deduced $\Delta S^{\text{o}}_{\text{ads}}$ value of -42.54 J mol^{-1} K^{-1} is very close to those obtained using the Eq. (25) (Table 6).
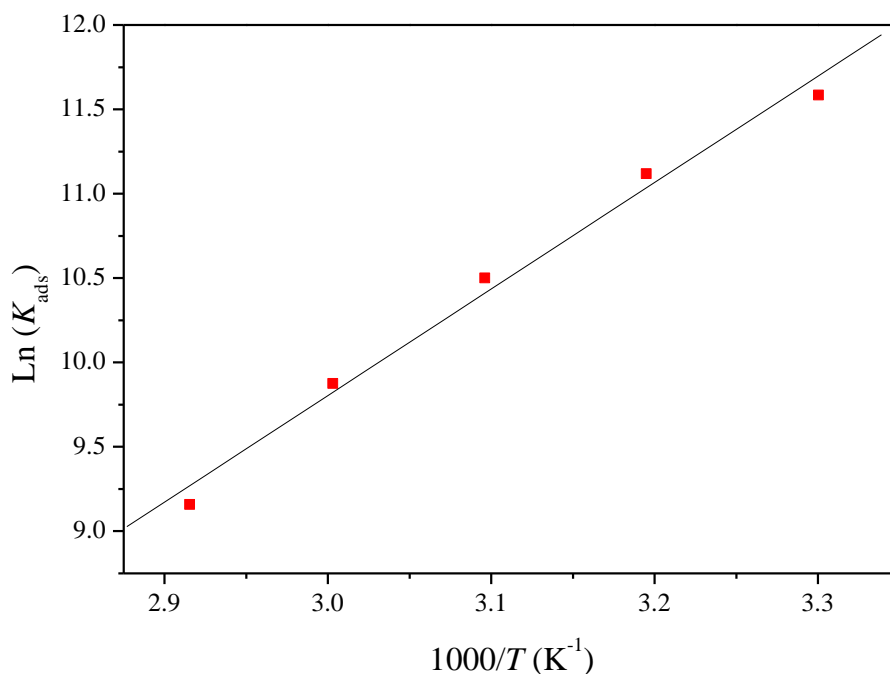
Figure 9. Vant't Hoff plot for the Copper/ABT/2M HNO$_3$ system.

4. CONCLUSION

From the overall experimental results and discussion, the following conclusions can be deduced:

> ➤   It was found that the 2-aminobenzenethiol (ABT) is effective inhibitor. The inhibitor efficiencies determined by weight loss, ac impedance and dc polarization methods are in reasonable agreement.

> ➤   Results showed that the inhibition efficiency was increased with increasing of concentration but decreases with rise temperature of ABT.

> ➤   Polarization curves revealed that the used inhibitor is mixed-type inhibitor.

> ➤   The surface adsorption of the used inhibitor led to a reduction in the double layer capacitance as well as an increase in the charge transfer resistance.

> ➤   The adsorption of ABT on the copper surface obeyed to Langmuir isotherm and it represented a mixture physical and chemical adsorption. The adsorption process is a spontaneous and exothermic process.

References

1.   I. Ahamad, R. Prasad, M.A. Quraishi, *Corros. Sci*. 52 (2010) 1472.
2.   A. K. Singh, M.A. Quraishi, *Corros. Sci*. 52 (2010) 152.
3.   L.R. Chauhan, G. Gunasekaran, *Corros. Sci*. 49 (2007) 1143.
4.   Y. Abboud, A. Abourriche, T. Saffaj, M. Berrada, M. Charrouf, A. Bannamara, N. Al-Himidi, H. Hannache, *Mater. Chem. Phys*. 105 (2007) 1.
5.   H. Zarrok, A. Zarrouk, R. Salghi, H. Oudda, B. Hammouti, M. Assouag, M. Taleb, M. Ebn Touhami, M. Bouachrine and S. Boukhris, *J. Chem. Pharm. Res*., 4 (2012) 5056.
6.   H. Zarrok, A. Zarrouk, R. Salghi, Y. Ramli, B. Hammouti, M. Assouag, E. M. Essassi, H. Oudda and M. Taleb, *J. Chem. Pharm. Res*., 4 (2012) 5048.
7.   L.B. Tang, G. N. Mu, G. H. Liu, *Corros. Sci*. 45 (2003) 2251.
8.   M. Bouklah, B. Hammouti, M. Lagrenée, F. Bentiss, *Corros. Sci*. 48 (2006) 2831.
9.   M.A. Quaraishi, D.D. Jamal, *Corrosion*. 56 (2000) 156
10. A. Zarrouk, M. Messali, M. R. Aouad, M. Assouag, H. Zarrok, R. Salghi, B. Hammouti, A. Chetouani, *J. Chem. Pharm. Res*., 4 (2012) 3427.
11. M. Elbakri, R. Touir, M. Ebn Touhami, A. Zarrouk, Y. Aouine, M. Sfaira, M. Bouachrine, A. Alami, A. El Hallaoui, *Res. Chem. Intermed*., (2012) DOI: 10.1007/s11164-012-0768-6.
12. L. Herrag, B. Hammouti, S. Elkadiri, A. Aouniti, C. Jama, H. Vezin, F. Bentiss, *Corros. Sci*. 52 (2010) 3042.
13. H. Bendaha, A. Zarrouk, A. Aouniti, B. Hammouti, S. El Kadiri, R. Salghi, R. Touzani, *Phys. Chem. News*, 64 (2012) 95.
14. L. Li, Q. Qu, W. Bai, F. Yang, Y. Chen, S. Zhang, Z. Ding. *Corros. Sci*. 59 (2012) 249.
15. 15.A. Ghazoui, R. Saddik, B. Hammouti, A. Zarrouk, N. Benchat, M. Guenbour, S. S. Al-Deyab, I. Warad, *Res. Chem. Intermed*., (2012) DOI: 10.1007/s11164-012-0763-y.
16. 16.P. Lowmunkhong, D. Ungthararak, P. Sutthivaiyakit. *Corros. Sci*. 52 (2010) 30.
17. 17.N. Soltani, M. Behpour, S.M. Ghoreishi, H. Naeimi. *Corros. Sci*. 52 (2010) 1351.
18. D. Ben Hmamou, R. Salghi, A. Zarrouk, M. Messali, H. Zarrok, M. Errami, B. Hammouti, Lh. Bazzi , A. Chakir, *Der Pharm. C*hem., 4 (2012) 1496.
19. G. Quartarone ., L. Ronchin, A. Vavasori, C. Tortato, L. Bonaldo. Corros. Sci. 64 (2012) 82.
20. S. E. Nataraja, T. V. Venkatesha, K. Manjunatha, B. Poojary, M. K. Pavithra, H.C. Tandon, Corros. Sci.53 (2011) 2651.
21. 21.H. Zarrok, H. Oudda, A. El Midaoui, A. Zarrouk, B. Hammouti, M. Ebn Touhami, A. Attayibat, S. Radi, R. Touzani, *Res. Chem. Intermed*., (2012) DOI: 10.1007/s11164-012-0525-x.

22. H. Zarrok, R. Salghi, A. Zarrouk, B. Hammouti, H. Oudda, Lh. Bazzi, L. Bammou, S. S. Al-Deyab, *Der Pharm. Chem.*, 4 (2012) 407.
23. A. Ghazoui, R. Saddik, N. Benchat, B. Hammouti, M. Guenbour, A. Zarrouk, M. Ramdani, *Der Pharm. Chem.*, 4 (2012) 352.
24. H. Zarrok, R. Saddik, H. Oudda, B. Hammouti, A. El Midaoui, A. Zarrouk, N. Benchat, M. Ebn Touhami, *Der Pharm. Chem.*, 3 (2011) 272.
25. H. Zarrok, A. Zarrouk, B. Hammouti, R. Salghi, C. Jama, F. Bentiss, *Corros. Sci.*, 64 (2012) 243.
26. B. Hammouti, A. Dafali, R. Touzani, M. Bouachrine. *Journal of Saudi Chemical Society* 16 (2012) 413.
27. A. Ostovari, S.M. Hoseinieh, M. Peikari, S.R. Shadizadeh, S.J. Hashemi, *Corros. Sci.*, 51 (2009) 1935.
28. A.K. Singh, M.A. Quraishi, *Corros. Sci.*, 52 (2010) 152.
29. S.K. Shukla, M.A. Quraishi, R. Prakash, *Corros. Sci.*, 50 (2008) 2867.
30. M.A. Quraishi, S.K. Shukla, *Mater. Chem. Phys.*, 113 (2009) 685.
31. G. Moretti, G. Quartarone, A. Tassan, A. Zingoles, *Electrochem. Acta,* 41 (1996) 1971.
32. G. Quartarone, G. Moretti, T. Bellomi, G. Capobianco, A. Zingales, *Corrosion,* 54 (1998) 606.
33. W.D. Bjorndahl, K. Nobe, *Corrosion,* 40 (1984) 82.
34. R. Schumacher, A. Muller, W. Stockel, *J. Electroanal. Chem.*, 219 (1987) 311.
35. W.H. Smyrl, in: J.O'M. Bockris, B.E. Conway, E. Yeager, R.E. White (Eds.), Comprehensive Treatise of Electrochemistry, vol. 4, Plenum Press, New York, 1981, p. 116.
36. P. Jinturkar, Y.C. Guan, K.N. Han, *Corrosion,* 54 (1984) 106.
37. E. Mattsson, J.O'M. Bockris, *Trans. Faraday Soc.*, 55 (1959) 1586.
38. G.G.O. Cordeiro, O.E. Barcia, O.R. Mattos, *Electrochim. Acta,* 38 (1993) 319.
39. D.K.Y. Wang, B.A.W. Coller, D.R. Macfarlane, *Electrochim. Acta,* 38 (1993) 2121.
40. R. Caban, T.W. Chapman, *J. Electrochem. Soc.* 124 (1977) 1371.
41. T. Hurlen, G. Ottesen, A. Staurset, *Electrochim. Acta,* 23 (1978) 23.
42. F. Bentiss, M. Lagrenee, M. Traisnel, J.C. Hornez, *Corrosion,* 55 (1999) 968.
43. H. Shih, H. Mansfeld, *Corros. Sci.* 29 (1989) 1235.
44. F. Bentiss, B. Mehdi, B. Mernari, M. Traisnel, H. Vezin, *Corrosion,* 58 (2002) 399.
45. E. McCafferty, N. Hackerman, *J. Electrochem. Soc.*, 119 (1972) 146.
46. M. Scendo, *Corros. Sci.*, 50 (2008) 1584.
47. K.F. Khaled, *Mater. Chem. Phys.*, 125 (2011) 427.
48. A. Zarrouk, B. Hammouti, H. Zarrok, S. S. Al-Deyab, I. Warad, *Res. Chem. Intermed.*, (2012) DOI: 10.1007/s11164-012-0492-2.
49. F. Mounir, S. El Issami, Lh. Bazzi, R. Salghi, L. Bammou, L. Bazzi, A. Chihab Eddine & O. Jbara. International Journal of Research and Reviews in Applied Sciences, 13 (2) (2012) 564.
50. B. Hammouti, A. Zarrouk, S.S. Al-Deyab and I. Warad*, Orient. J. Chem.*, (2011) 23.
51. F. Bentiss, C. Jama, B. Mernari, H. El Attari, L. El Kadi, M. Lebrini, M. Traisnel, M. Lagrenée. *Corros. Sci.* 51 (2009) 1628.
52. S.A.M. Refaey, F. Taha, A.M. Abd El-Malak, *Appl. Surf. Sci.*, 236 (2004) 175.
53. I. N. Putilova, S. A. Balezin, V. P. Barannik, Metallic Corrosion Inhibitors; Pergamon Press Ltd.: Oxford, 1960.
54. H. Ashassi-Sorkhabi, B. Shabani, B. Aligholipour, D. Seifzadeh, *Appl. Surf. Sci.*, (2006) 4039.
55. N. O Eddy, E. E. Ebenso. *Pigment & Resin Technology*, 39 (2) (2010) 77.
56. G. Moretti, F. Guidi, G. Grion, *Corros. Sci.*, 46 (2004) 387.
57. A. Popova, E. Sokolova, S. Raicheva, M. Christov, *Corros. Sci.*, 45 (2003) 33.
58. K.C. Emregul, M. Hayvali, *Corros. Sci.*, 48 (2006) 797.
59. M. Behpour, S.M. Ghoreishi, N. Soltani, M. Salavati-Niasari, M. Hamadanian, A. Gandomi, *Corros. Sci.*,50 (2008) 2172.
60. M. Lagrenee, B. Mernari, M. Bouanis, M. Traisnel, F. Bentiss, *Corros. Sci.*, 44 (2002) 573.

61. F.M. Donahue, K. Nobe, *J. Electrochem. Soc*., 112 (1965) 886.
62. I. Ahamad, M.A. Quraishi, *Corros. Sci*., 52 (2010) 651.
63. F. Bentiss, M. Lebrini, M. Lagrenee, *Corros. Sci*., 47 (2005) 2915.
64. F. Bentiss, M. Lagrenee, M. Traisnel, J.C. Hornez, *Corros .Sci*., 41 (1999) 789.
65. E.A. Noor, A.H. Al-Moubaraki, *Mater. Chem. Phys*., 110 (2008) 145.
66. R. Arshadi, M. Lashgari, Gh. A. Parsafar, *Mater. Chem. Phys.,* 86 (2004) 311.